



## PERFORMANCE BASED OPTIMAL SEISMIC DESIGN OF RC SHEAR WALLS INCORPORATING SOIL–STRUCTURE INTERACTION USING CSS ALGORITHM

A. Kaveh<sup>\*,†</sup> and P. Zakian

*Centre of Excellence for Fundamental Studies in Structural Engineering, Department of  
Civil Engineering, Iran University of Science and Technology, Tehran-16, Iran*

### ABSTRACT

In this article optimal design of shear walls is performed under seismic loading. For practical aims, a database of special shear walls is created. Special shear walls are used for seismic design optimization employing the charged system search algorithm as an optimizer. Constraints consist of design and performance limitations. Nonlinear behavior of the shear wall is taken into account and performance based seismic design optimization is accomplished. Capacity curves of the optimal solution are determined and compared incorporates soil–structure interaction. Also an optimization based method is proposed for bilinear approximation of capacity curve. These are a new methodology for seismic RC shear wall optimum design.

Received: 20 February 2012; Accepted: 20 June 2012

**KEY WORDS:** charged system search; shear wall; seismic design; structural optimization; soil-structure interaction; nonlinear static analysis

### 1. INTRODUCTION

Optimization in design of structures is usually implemented to nomination the variables so as to attain an optimum structural weight or cost, whereas the design criteria are satisfied. In

---

\* Corresponding author: A. Kaveh, Centre of Excellence for Fundamental Studies in Structural Engineering, Department of Civil Engineering, Iran University of Science and Technology, Tehran-16, Iran

† E-mail address: alikaveh@iust.ac.ir (A. Kaveh)

contrast to steel structures, optimizing RC structures is more complex. The main reason for this problem is semi-infinite set of member sizes and various templates of reinforcement [1]. In concrete structures, at least three different cost items should be considered in the optimization process consisting of costs of concrete, steel, and the formwork [2].

Walls that primarily resist lateral loads due to the wind or earthquakes acting on the building are called shear walls or structural walls. These walls often provide lateral bracings for the rest of the structure. They withstand gravity loads transferred to the wall by the components of the structure tributary to the wall, in addition to lateral-loads (lateral shear forces) and moments about the strong axis of the wall [3]. Design codes emphasize that in the regions with medium or high seismic risk level, special reinforcement is required in order to have favorable performance of concrete structures against earthquake hazards [4]. Regions comprising of concentrated and tied reinforcement are known as boundary elements, irrespective of whether or not they are thicker than the rest of the wall.

There are some publications on seismic design of shear walls. Wallace [5, 6] proposed new code format for seismic design of RC structural walls, Sasani [7] proposed a performance design methodology relative to concrete structural walls. The performance level targeted in the design was life safety. Kowalsky [8] presented RC structural walls designed according to UBC and displacement-based methods.

Many researchers have addressed the optimum design of seismic structures, but a few works exist on optimal design of shear walls incorporating new seismic codes' considerations. Saka [9] offered Optimum design of multistory structures with shear walls, Ganzerli et al. [10] presented a performance-based design using structural optimization. The optimum design of active seismic structures was studied by Cheng and Pantelides [11]. Fragiadakis et al. [12] carried out performance-based optimum seismic design of structural reinforced concrete structures.

The three performance levels are defined as follows:

(i) Collapse Prevention level (CP): the building is not collapsed only; any other damage or loss is admissible; (ii) life Safety level (LS): the structure remains stable and has meaningful capacity save; hazardous nonstructural damage is controlled; and (iii) Immediate Occupancy level (IO): the building is safe to inhabit, any repairs are minor.

In structural earthquake engineering considering Soil-Structure Interaction (SSI) is often a vital phase of analysis and design of the structures. For example when designing slender structures such as tall buildings or bridge piers, it is necessary to incorporate the features of the soil [13]. Some of the first studies on soil-structure interaction that used the analytical and experimental results from elastic half-space theory were performed by Hall [14], Parmelee [15] and Parmelee et al. [16]. Although the main limitation was the dependency of the impedance on the exciting frequency, these became the first attempts to establish a link between the elastic half space theory and the mass-spring-dashpot system [17]. Ghersi et al. [18] investigated the non-linear moment-rotation relationship at the base of the shear walls. Raychowdhury [19] carried out seismic response of low-rise steel moment-resisting frame buildings incorporating nonlinear soil-structure interaction.

In this article optimal design of shear walls is performed under seismic loading. For practical aims a database of special shear walls is created. Special shear walls are used for seismic design optimization and charged system search algorithm is employed for this

purpose. Constraints consist of design and performance criteria. Nonlinear behavior of the shear wall is taken into account and a performance based seismic design optimization is accomplished. Capacity curves of the optimum solution incorporating soil–structure interaction are determined and compared. For considering the inertial effects only, FEMA-356 [20] recommends to estimate: Initial stiffness and ultimate load capacity, here the first method of FEMA is used. Also a simple optimization formulation is proposed for bilinear approximation of capacity curve. This is a new methodology for seismic RC shear wall optimal design. The results show the usefulness of this practical optimization approach.

## 2. CONSTRUCTION OF DATABASE FOR SHEAR WALLS

In some recent investigations, for practical optimization of RC frames, discrete database of column and beam are constructed [1, 21]. Here, a database of special shear walls (a shear wall containing boundary elements) is created. Limitations are considered as:

- The  $l_w = h_w + 2 * t_f$  is the length of shear wall which is equal to 6.7 m.
- $200 < t_w < 400$  mm is assumed as the limitation for thickness.
- $600 < t_f < 1200$  mm is assumed as the limitation for length of the flange.
- $200 < b_f < 1200$  mm is assumed as the limitation for width of the flange.
- $300 < S_{sh} < 450$  mm based on ACI 318-08[22] code is the distance of the vertical and horizontal shear bars which are considered identical in order to reduce the discrete section numbers. Diameter of these bars is taken as 16 mm.

$\Phi_{be}$  is the diameter of each bar of the flange (boundary element) that is selected as 32 or 36 mm.

Intervals of the dimensions is considered as 100 mm, and intervals of the  $S_{sh}$  is considered as 50 mm.

$A_{sf \min} = 0.01 * t_f * b_f$  is the minimum reinforcement area of one flange.

$A_{sf \max} = 0.04 * t_f * b_f$  is the maximum reinforcement area of one flange.

These formulations are proposed for boundary element reinforcement arrangement:

$$nw_1 = 2Int\left(\frac{b_f - 2(t_c + d_t) + s_c}{d_b + s_c} - 0.5\right) \tag{1a}$$

$$nw_2 = 2Int\left(\frac{b_f - 2(t_c + d_t) + s_c}{d_b + s_c} + \frac{t_f - 2(t_c + d_t) + s_c}{d_b + s_c} - 0.5\right) \tag{1b}$$

$$nrl_{\min} = \max\left(Int\left(\frac{b_f}{t_f + b_f} \times \frac{A_{sf \min}}{a_s} + 0.5\right), 4\right) \tag{1c}$$

$$nrl_{\max} = \min(\text{Int}(\frac{b_f}{t_f + b_f} \times \frac{A_{sf \max}}{a_s} - 0.5), nw_1) \tag{1d}$$

$$nud_{\min} = \max(\text{Int}(\frac{A_{sf \min}}{a_s} + 0.5), 4) - nrl_{\min} \tag{1e}$$

$$nud_{\max} = \min(\text{Int}(\frac{A_{sf \max}}{a_s} - 0.5), nw_2) - nrl_{\max} \tag{1f}$$

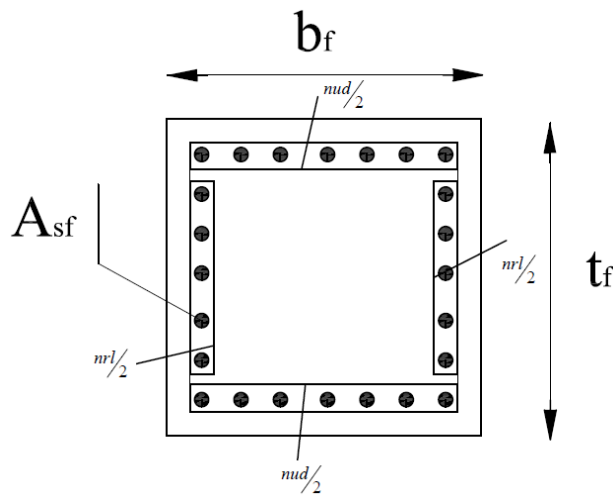


Figure 1. Reinforcement notations of the boundary element

$nud$  and  $nrl$  are the number of bars defined in Figure 1.  $a_s$  is the area of selected reinforcement bars of the boundary elements.  $d_b$  is the flexural reinforcing bar diameter;  $d_t$  is the diameter of tie bar;  $s_c$  is spacing between longitudinal bars in the boundary element;  $t_c$  is the cover thickness;  $\text{Int}(x)$  rounds to integer part of the  $x$ .

Note that each value which is selected for  $nrl$  and  $nud$  must be an even number, and if any one is an odd number, then it must be round to the nearest even number in its allowable domain.

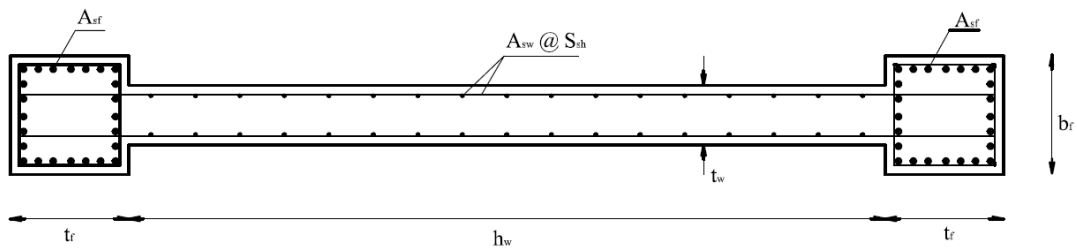


Figure 2. Topology of a special shear wall section

Figure 2 shows the topology and notations of the considered special shear wall cross-section. The created shear wall section database is provided in Table 1 containing 7568 wall sections being generated for discrete optimization.

Table 1. Section data base of the special shear wall

No.	$t_w$	$t_f$	$b_f$	$S_{sh}$	$\Phi_{be}$	$N_{rl}$	$N_{ud}$
1	200	600	400	500	32	4	6
2	200	600	400	350	32	4	6
3	200	600	400	400	32	4	6
4	200	600	400	450	32	4	6
----	----	----	----	----	----	----	----
3290	300	700	1100	300	36	14	8
3291	300	700	1100	300	36	16	10
3292	300	700	1100	300	36	18	10
3293	300	700	1100	300	32	6	4
----	----	----	----	----	----	----	----
7565	400	1200	1200	400	36	20	20
7566	400	1200	1200	400	36	22	22
7567	400	1200	1200	400	36	24	24
7568	400	1200	1200	400	36	26	26

### 3. FORMULATION OF SPECIAL SHEAR WALL SEISMIC DESIGN OPTIMIZATION

Cost of the shear wall includes the cost of concrete, steel bars and formwork. Cost of the special transversal reinforcement at the base of the shear wall, is neglected because of small effect on the total cost function.

Optimization constraints consist of design constraints and performance constraint, i.e. plastic rotation limitation. An optimization problem in general form can be defined as:

$$\begin{aligned}
& \text{Minimize } f(X) \\
& \text{subject to } g_i(X) \leq 0 \\
& X = [x_1, x_2, \dots, x_{ng}] \\
& i = 1, 2, \dots, ng \\
& x_i \in R^d
\end{aligned} \tag{2}$$

Database sections are sorted by their cost per unit height of the wall, and  $X$  is the solution vector containing the cost per unit height of wall, and  $ng$  is the number of design variable or the number of member groups.  $R^d$  is the design domain of the variables.

$$\text{to minimize } \text{fit}(X) = f(X) \times f_{\text{penalty}}(X) \tag{3}$$

Where  $\text{fit}(X)$  is the fitness function,  $f(X)$  is the objective function which is the cost of the shear wall,  $f_{\text{penalty}}(X)$  is penalty function utilized for constraint handling:

$$f = \text{concrete cost} + \text{steel cost} + \text{formwork cost} \tag{4}$$

$$\text{Concrete cost} = C_c * (2 * b_f * t_f * H_w + h_w * t_w * H_w - 2 * m_1 * A_{sf} - m_2 * A_{sw}) \tag{5a}$$

$$\text{Steel cost} = \gamma_{st} * C_{st} * ((2 * m_1 * A_{sf} + m_2 * A_{sw}) * H_w + 2 * l_w * \text{Int}(H_w / S_{sh}) * A_{sw}) \tag{5b}$$

$$\text{Formwork cost} = C_f * (4 * (b_f + t_f - 0.5 * t_w) * H_w + 2 * h_w * H_w) \tag{5c}$$

$H_w$  is the total height of the wall;  $A_{sf}$  is cross-section area of each bar in the flange of the wall;  $A_{sw}$  is the cross-section area of each bar in the web of the wall, for longitudinal and transversal shear reinforcement considered as one cross-section area;  $h_w$  is the length of the shear wall's cross-section web;  $m_1$  is the number of reinforcement bars in each flange;  $m_2$  is the number of reinforcement bars in the web.

Constant values:  $C_c = 60 \$/m^3$  is the unit cost of the concrete;  $C_s = 0.9 \$/kg$  is the unit cost of the steel;  $C_f = 18 \$/m^2$  is the unit cost of the formwork;  $\gamma_s = 7850 kg/m^3$  is the density of the steel;

Penalty approach is used for constraint handling.

$$f_{\text{penalty}}(X) = (1 + \varepsilon_1 \cdot \nu)^{\varepsilon_2}, \quad \nu = \sum_{i=1}^n \max[0, v_i] \tag{6}$$

In this paper, the parameters  $\varepsilon_1$  and  $\varepsilon_2$  for the penalty function, are chosen as 1 and 2, respectively.  $\nu$  is the sum of the disapproval constraints.

Optimization constraints are defined as follows:

Plastic rotation limitation is considered as a performance constraint and imposed on the

first level (story) of the shear wall including four checkpoint sections, because initial plastic hinges are formed at places near the base of the wall. In order to calculate the plastic rotations, after each nonlinear static (pushover) analysis, the moment-curvature data of the checkpoints are obtained and ultimate curvature  $\phi_u$  is specified for each checkpoint, then this equation can be utilized:

$$\theta_p = (\phi_u - \phi_y)L_p \quad (7)$$

$\theta_p$  is the plastic rotation,  $\phi_y$  is the yield curvature which is defined as Ref. [8]:

$$\phi_y = \frac{0.003}{l_w} \quad (8a)$$

$L_p$  is the assumed plastic hinge length:

$$L_p = \frac{l_w}{2} \quad (8b)$$

Based on FEMA criteria [20] allowable plastic rotation  $\theta_{pall}$  of shear walls that are controlled by flexure for the *IO*, *LS* and *CP* performance levels are 0.005, 0.010 and 0.015, respectively. In this study IO level is utilized for optimization procedure, and thus it is equal to  $\theta_{pall} = 0.005$ .

Plastic rotation constraint is shown in Eq. (9):

$$g_1 = \frac{\theta_p}{\theta_{pall}} - 1 \leq 0 \quad (9)$$

For seismic design of special shear wall [3, 4] some important design constraint must be used.  $c$  is compression region length of the wall section. The ACI 318-08 [22] express these restrictions for design as:

$$c \geq \frac{l_w}{600 \left( \frac{\delta_u}{H_w} \right)} \quad \text{such that} \quad \frac{\delta_u}{H_w} \geq 0.007 \quad (10a)$$

$\delta_u$  is the design displacement. In this paper for risk category of IV it is equal to  $0.0045H_w$  based on the ASCE 7-10 [23]. Wallace [5] has provided the following relationship for the calculation of  $c$  as:

$$c = \left( \frac{\left( \left( \rho + \rho'' - \frac{\gamma}{\alpha} \rho' \right) \frac{\alpha f_y}{f_c'} + \frac{P}{A_w f_c'} \right)}{0.85 \beta_1 + 2 \rho'' \frac{\alpha f_y}{f_c'}} \right) l_w \quad (10b)$$

Eq. (10b) can be used for the maximum compressive strain of  $\varepsilon_{c\max} \leq 0.005$  and  $c \leq 0.5l_w$  more detail about these parameters can be found in Ref. [5].

Minimum length of each flange is:

$$t_{f\min} = \max\{c - 0.1l_w, c/2\} \quad (10c)$$

The second constraint is a limitation for the flange length:

$$g_2 = \frac{t_f}{t_{f\min}} - 1 \geq 0 \quad (11)$$

Ultimate shear strength of the wall is defined as:

$$V_{u\max} = \phi_v V_{n\max} = \frac{2}{3} \phi_v \sqrt{f'_c} A_{cv} \quad A_{cv} = t_w \times l_w \quad (12)$$

Shear force of the wall  $V_u$  must be controlled by the nominal shear strength  $V_{n\max}$ . This restriction can be expressed as:

$$g_3 = \frac{V_u}{V_{u\max}} - 1 \leq 0 \quad (13)$$

Here, the shear force demand of the wall,  $V_u$ , is selected greater than  $\frac{1}{6} \sqrt{f'_c} A_{cv}$ .

Therefore, according to the ACI at least in double layer shear reinforcement in both orthogonal directions of wall must be used. Special reinforcement of wall is determined in the following form:

$$V_n = \frac{V_u}{\phi_v} = A_{cv} (\alpha_c \sqrt{f'_c} + \rho_{ta} f_y) \quad (14)$$

$\rho_{ta}$  is the required transversal shear reinforcement ratio of the wall obtained from Eq. (14).

Here,  $V_u$  is greater than  $\frac{1}{12} \sqrt{f'_c} A_{cv}$ , thus  $\rho_{t,\min} = \rho_{l,\min} = 0.0025$ .  $\rho_{l,\min}$  is the minimum longitudinal shear reinforcement ratio.

After determining of  $\rho_{ta}$  from Eq. (14), based on the existence reinforcement ratio  $\rho_t$ :

The transversal shear reinforcement ratio constraint is:

$$g_4 = \frac{\rho_t}{\rho_{ta}} - 1 \geq 0 \quad (15)$$



Considering the combination of axial force  $P_u$  and bending moment  $M_u$  demands is necessary in the design of wall. Due to tall height of the wall and neglecting the longitudinal (vertical) shear reinforcement, with good approximation we can convert the moment to a couple of compressive force  $C_u$  and tension force  $T_u$  [3, 4]. Hence, we can design flanges such as a column by these force demands:

$$T_u = \frac{M_u}{z} \quad (16a)$$

$$C_u = P_u + \frac{M_u}{z} \quad (16b)$$

$T_{ua}$ ,  $C_{ua}$  are allowable tension and compressive forces, respectively;  $z$  is the distance between the center of two flanges.

$$T_{ua} = \phi_t A_s f_y \quad (16c)$$

$$C_{ua} = \phi_c [0.85 f'_c (A_g - A_{st}) + A_{st} f_y] \quad (16d)$$

$\phi_v$ ,  $\phi_t$  and  $\phi_c$  are the strength reduction factors being equal to 0.75, 0.90 and 0.65 according to the ACI, respectively;  $f'_c$  is the compressive strength of concrete and  $f_y$  is the yield stress of steel;

Tension and compressive strength constraints are as follows:

$$g_5 = \frac{T_u}{T_{ua}} - 1 \leq 0 \quad (17)$$

$$g_6 = \frac{C_u}{C_{ua}} - 1 \leq 0 \quad (18)$$

All together we have six constraints for shear wall design optimization.

### 3. PERFORMANCE BASED CONCEPTS FOR DESIGN

Convex model approach [24] is employed for considering seismic excitation and period uncertainties of the shear wall. Using the convex model is not essential, and if the period of the structure is assumed, then designer can use the maximum valid earthquake response spectra directly. The structural response to an uncertain earthquake can be appraised in the convex domain. The convex model theory can determine the maximum response of the structure, without determining the response of every point in the convex zone. The convex model theory establishes that the maximum response in a convex zone can be found on the convex hull (the closed external perimeter) of the convex set. This model is proposed by

Ganzerli et al. [10] for a portal frame. The convex region is shown by the closed area between the dashed lines and design spectrums, Figure 3.

Middle period for these shear walls in the database is 0.65 sec for initial design. To find the boundaries of the convex model, it is supposed that the shear wall has a deviation from the nominal stiffness equal to 50 percent, and a deviation from the nominal mass of 10 percent. These deviations are estimated by using the data of existing shear walls. For simplicity the upper bound and lower bound values of the period can be calculated by the period of a single degree of freedom system. This period is obtained from Eq. (19):

$$T = 2\pi \sqrt{\frac{m}{K}} \quad (19)$$

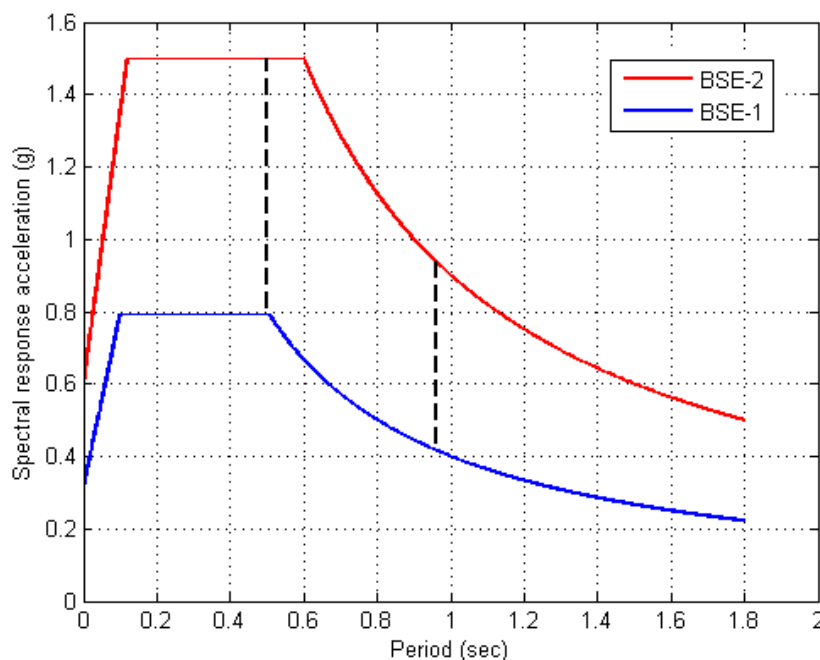


Figure 3. Design spectra and convex region

For the above referenced range of variations from the nominal values of the mass  $m$  and the structural stiffness  $K$  of the considered shear walls, the period varies between 0.50 and 0.96 sec. The specific geographical area is chosen as Ref [10], and the acceleration parameters obtained from the maps provided with the following guidelines are as follows: For the BSE-1,  $S_s = 0.6$  g, and  $S_l = 0.2$  g. For the BSE-2,  $S_s = 1.50$  g, and  $S_l = 0.6$  g. Here, BSE is the abbreviation for Basic Safty Earthquake (for further description see Ref. [20]). The acceleration parameters must be modified to account for the site class effects and are used to construct the design spectrum. The adjustment for site class can be obtained by using the following expressions:

$$S_{XS} = F_a S_s \quad (20a)$$

$$S_{x1} = F_v S_1 \quad (20b)$$

A general horizontal response spectrum as shown in Figure 3 should be developed using the following equations:

$$S_a = S_{xs} \left[ \left( \frac{5}{B_s} - 2 \right) \frac{T}{T_s} + 0.4 \right] \quad \text{for} \quad 0 < T < T_0 \quad (20c)$$

$$S_a = S_{xs} / B_s \quad \text{for} \quad T < T_s \quad (20d)$$

$$S_a = S_{x1} / B_1 T \quad \text{for} \quad T > T_s \quad (20e)$$

More details on the above equations can be found in Ref [20].

The provisions [20] give a relationship for estimating the target displacement  $\delta_t$  using the following expression:

$$\delta_t = C_0 C_1 C_2 C_3 S_a \frac{T^2}{4\pi^2} g \quad (21)$$

$C_0$  is a modification factor to relate the spectral displacement of an equivalent SDOF system to the roof displacement of the MDOF system. Here  $C_0$  is equal to 1.3.  $C_1$  is a modification factor to relate the expected maximum inelastic displacements to the calculated linear elastic response displacements;  $C_1$  is equal to 1.0 for this structure.  $C_2$  is the modification factor to represent the effect of pinched hysteretic shape, stiffness degradation and strength deterioration on maximum displacement response for *IO* level and for this structure it is considered as 1.0.  $C_3$  is the modification factor to represent the increased displacements due to dynamic  $P - \Delta$  effects. For buildings with positive post-yield stiffness, this is equal to 1.0.  $S_a$  is the response spectrum acceleration, at the effective fundamental period and damping ratio of the building in the direction under consideration, and  $g$  is the acceleration of gravity. Target displacement for the BSE-2 earthquake ( $S_a = 1.5 g$ ) is calculated as 205 mm. Hence, the upper bound condition is used for the shear wall nonlinear static analysis.

## 4. CHARGED SYSTEM SEARCH

### 4.1. Definition of charged system search

Charged system search was proposed by Kaveh and Talatahari [25]. This algorithm is based on Gauss and Coulomb laws from electrostatics and the Newtonian laws of classic mechanics. The CSS is a population based algorithm, where each agent is called a charged

particle (CP) that is supposed to be a sphere with radius of  $a$  which has uniform charge distribution. Each CP is under the influence of other particle's force field. The value of the resultant force is specified by using the electrostatics laws and the quality of the movement is determined using the Newtonian mechanics laws. A good CP induces more force than the bad ones. The main steps in this algorithm are as follows:

Step 1: Initialization. The initial positions or arrays of CPs are specified randomly in the search domain and the initial velocities of the CPs are supposed to be zero. The values of the objective function for the CPs are specified and the CPs are sorted in an increasing order. The best CP among the whole set of CPs will be recorded as  $X_{best}$  and its related objective function value is shown by  $fit_{best}$ . Similarly, the worst CP is recorded as  $fit_{worst}$ . A number of the first CPs and their related values of the objective function are stored in a memory, known as the charged memory (CM).

$$x_{i,j}^0 = x_{i,\min} + rand \cdot (x_{i,\max} - x_{i,\min}), \quad i = 1, 2, \dots, N \quad (22)$$

$$CM = \lfloor x_{i,j} \rfloor_{N \times CMS} \quad (23)$$

$N$  is the number of variables, CMS is the charged memory size that is usually equal to the integer part of the  $(Number\ of\ CPs)/4$ .  $x_{i,\max}$  and  $x_{i,\min}$  are upper bound and lower bound of variable values  $i$ , respectively.  $rand$  is a random number with uniform distribution in the range of  $[0,1]$ .

Step 2: Forces calculation. Determine the force vector for each CP as

$$F_j = \sum_{i,i \neq j} \left( \frac{q_i}{a^3} r_{ij} \cdot i_1 + \frac{q_i}{r_{ij}^2} \cdot i_2 \right) p_{ij} (X_i - X_j) \quad \begin{cases} j = 1, 2, \dots, N \\ i_1 = 1, \quad i_2 = 0 \Leftrightarrow r_{ij} < a \\ i_1 = 0, \quad i_2 = 1 \Leftrightarrow r_{ij} \geq a \end{cases} \quad (24)$$

Where  $F_j$  is the resultant force acting on the  $j$ th CP;  $N$  is the number of CPs. The value of charge for each CP,  $q_i$ , is defined considering the feature of its solution as

$$q_i = \frac{fit(i) - fit_{worst}}{fit_{best} - fit_{worst}} \quad i = 1, 2, \dots, N \quad (25)$$

Where  $fit_{best}$  and  $fit_{worst}$  are the best and the worst fitness of all the particles, respectively;  $fit(i)$  illustrates the fitness of the agent  $i$ . The distance  $r_{ij}$  between two charged particles is defined as follows:

$$r_{ij} = \frac{\|X_i - X_j\|}{\|(X_i + X_j)/2 - X_{best}\| + \varepsilon} \quad (26)$$

Where  $X_i$  and  $X_j$  are the positions of the  $i$ th and  $j$ th CPs, respectively,  $X_{best}$  is the position of the best current CP, and  $\varepsilon$  is a small positive value to avoid singularities. Here,  $p_{ij}$  is the probability criteria of moving each CP towards the others and is attained using the function as follows:

$$p_{ij} = \begin{cases} 1 & \frac{fit(i) - fit_{best}}{fit(j) - fit(i)} > rand \vee fit(j) > fit(i) \\ 0 & else \end{cases} \quad (27)$$

A suitable value for  $a$  is expressed considering the size of the search domain as

$$a = c_0 * \max(\{x_{i,max} - x_{i,min} | i = 1, 2, \dots, ng\}) \quad (28)$$

$c_0$  is a constant coefficient. In this paper a value near to 0.01 leads to a good solution.

Step 3: Moving of particles. Each CP moves to its new position and this new position is a function of old position and old velocity, new position and new velocity are calculated as

$$X_{j,new} = Fix(rand_{j1} \cdot k_a \cdot F_j + rand_{j2} \cdot k_v \cdot V_{j,old} + X_{j,old}) \quad (29)$$

$$V_{j,new} = X_{j,new} - X_{j,old} \quad (30)$$

Where  $k_a$  is the acceleration coefficient;  $k_v$  is the velocity coefficient; and  $rand_{j1}$  and  $rand_{j2}$  are two random numbers uniformly distributed in the range of (0,1);  $Fix(X)$  is a function which rounds each elements of  $X$  to the nearest permissible discrete value existing in the database [26].  $k_v$  controls the exploration process so it must be decreased for convergence,  $k_a$  controls exploitation process that is a parameter related to attractive force. Small values of this parameter lead to divergence or increasing of the computational time.  $k_v$  and  $k_a$  are linearly varying increasing and decreasing functions, respectively [25, 27].

Step 4: Updating procedure. If a new CP exits from the allowable search domain, a harmony search-based handling approach can be utilized to adjust its position [25]. According to this mechanism, any element of the solution vector violating the variable boundaries can be reproduced from the CM or from randomly selecting one value from the allowable range of values. Furthermore, if some new CP vectors are better than the worst ones in the CM, they are substituted with the worst ones in the CM.

Step 5: Terminating criterion check. Steps 2–4 should be repeated up to a terminating criterion is satisfied.

#### 4.2. Main rules of the charged system search

In this part some rules corresponding to the CSS are introduced. The rules are as follows [27]:

Rule 1: The CSS is a population-based algorithm. In each iteration, a predetermined number of agents are used to seek the search domain and the value of the charge for each agent or CP, and the distance between two charged particles is expressed by Eqs. (25) and (26).

Rule 2: The initial positions of the CPs are determined randomly by Eq. (22) in the

search space and the initial velocities of the charged particles are assumed to be zero.

Rule 3: Electric forces between any two CPs are supposed to be attractive force.

Rule 4: All good CPs can attract the bad CPs and only some of the bad particles can attract good particles, considering the probability criteria (Eq. (27)).

Rule 5: The value of the resultant electrical force affecting a CP is calculated using Eq. (24).

Rule 6: The new position and the new velocity of each CP are specified by Eqs. (29) and (30).

Rule 7: The CSS uses a memory (CM) which stores the best CP solution vectors and their corresponding objective function values.

Rule 8: The particles violating the boundaries of the variables are reproduced using the harmony search-based handling approach.

Rule 9: Terminating criterion

Here, a limited number of iteration is selected as a terminating criterion for fulfilling the process.

## 5. NUMERICAL EXAMPLE

In this section, the CSS algorithm is used for discrete optimization problem of special shear wall. Because of practical aims and constraint reduction of the problem, a shear wall section database is constructed. Six constraints are imposed to the problem containing five seismic design constraint and one performance constraint. Plastic rotation constraint often is not violated in the optimization process for three reasons as: The first is the implementation of five effective constraint. The second is because of using ACI code special criteria for creating database. The third is that the target displacement is based on the middle values of the convex region so it is maybe small for shear walls with strong sections.

Table 2. Definition of material properties in OpenSees

Concrete				
Material type	$f'_c$	$\epsilon_{c0}$	$f'_{cu}$	$\epsilon_{c0}$
Core concrete (confined)	25		0.0	
Uniaxial Material Concrete 01	MPa	0.002	MPa	0.0035
Cover concrete (unconfined)	25		5.0	
Uniaxial Material Concrete01	MPa	0.0024	MPa	0.006
Steel				
Material type	$f'_c$	$E_0$	$b$	
Reinforcing steel	400	200000		
Uniaxial Material Steel01	MPa	MPa	0.02	

Height of the shear wall is 42 m and its length is 6.7 m, height of each story is 3.5 m. Loading details and topology of 12 story shear wall are provided in Figure 4. MATLAB [28] and OpenSees [29] softwares are utilized for optimization and analysis procedure, respectively. For analysis phase in OpenSees, twelve nonlinear beam-column elements with distributed plasticity are applied for shear wall modeling, each element is divided by four

sections (integration points) and deformations of each section in the first story of the shear wall are recorded. Then plastic rotations are calculated using Eq. (7). Nonlinear concrete and steel material properties are provided in Table 2. As it is mentioned in this table the effects of confinement and unconfined parts of the wall fiber section are imposed in concrete properties definition. More information about the definition of materials can be found in Ref. [30].

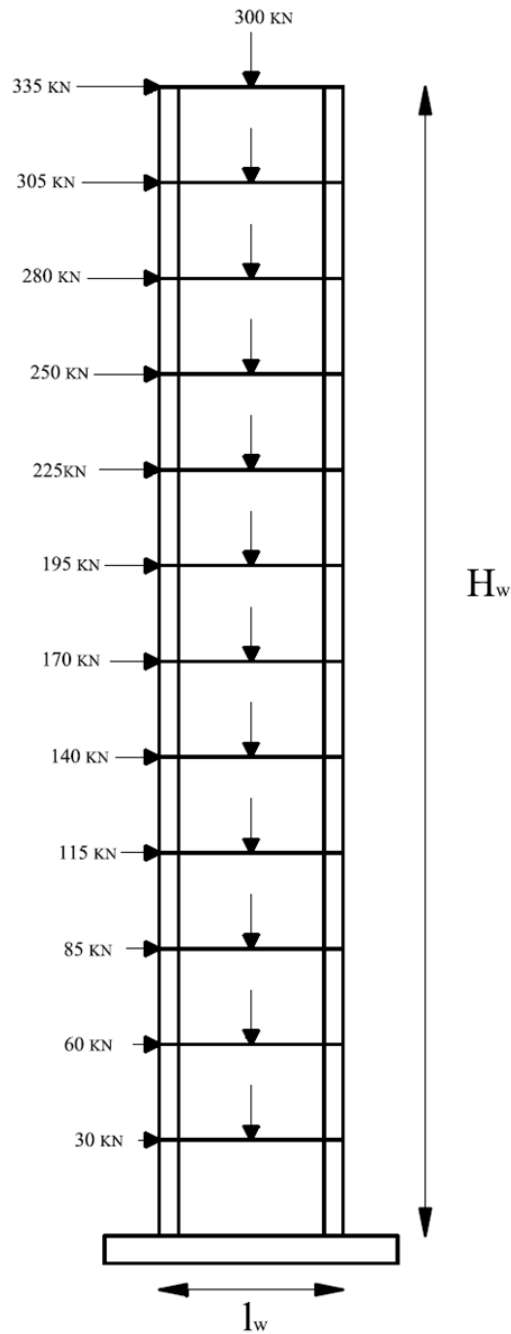


Figure 4. A special shear wall loading

Also, the P-Delta effects are included as a geometric transformation. Thus both material and geometry nonlinearity are considered.  $M_u, V_u, P_u$  are demand moment and forces at base of structure that are clarified by the loading forces. Optimum solution is provided in Table 3.

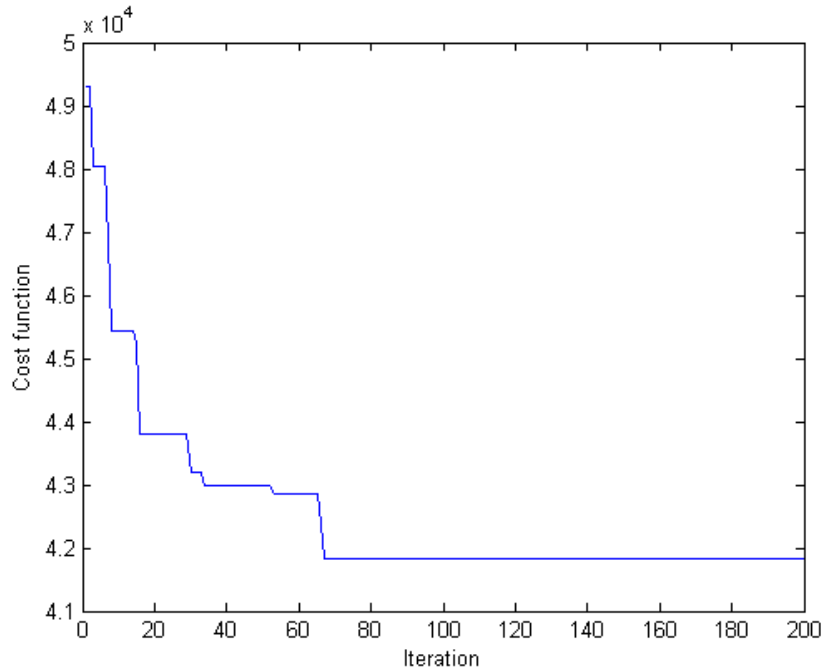


Figure 5. Convergence history of the CSS algorithm

Table 3. Optimum section properties and cost of the special shear wall

Cost (\$)	$t_w$ (m)	$t_f$ (m)	$b_f$ (m)	$S_{sh}$ (m)	$\Phi_{be}$	$N_{rl}$	$N_{ud}$
41831	0.30	1.20	0.80	0.45	32	16	24

Progress curve of the CSS is shown in Figure 5. Pushover curve of the optimum solution and plastic hinge formation sequence are plotted in Figure 6. First plastic hinge is formed in the first checkpoint section of the shear wall, which is in the first story and have a position with lowest height. The second and third plastic hinges are formed in the second and third section of the first story. Checkpoint sections (i.e. integration points of each element) for the first level are only recorded so as to calculate the plastic hinge rotations and are numbered from lower height. In Figure 7 plastic rotation limitations for three performance levels of optimum shear wall are shown on the capacity curve. Allowable plastic rotation for shear walls which are controlled by the flexure as to Immediate Occupancy level (IO), Life Safety level (LS) and Collapse Prevention (CP), are defined as 0.005, 0.010 and 0.015, respectively.



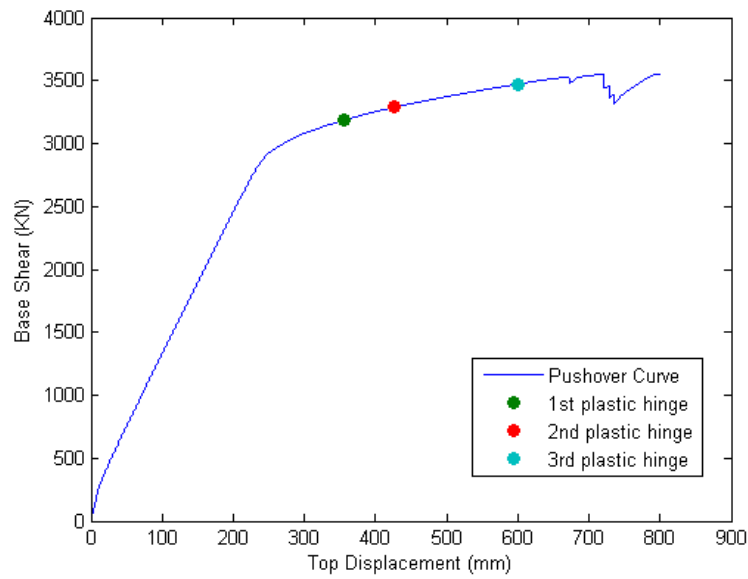


Figure 6. The capacity curve of the optimum solution: plastic hinge formation sequence

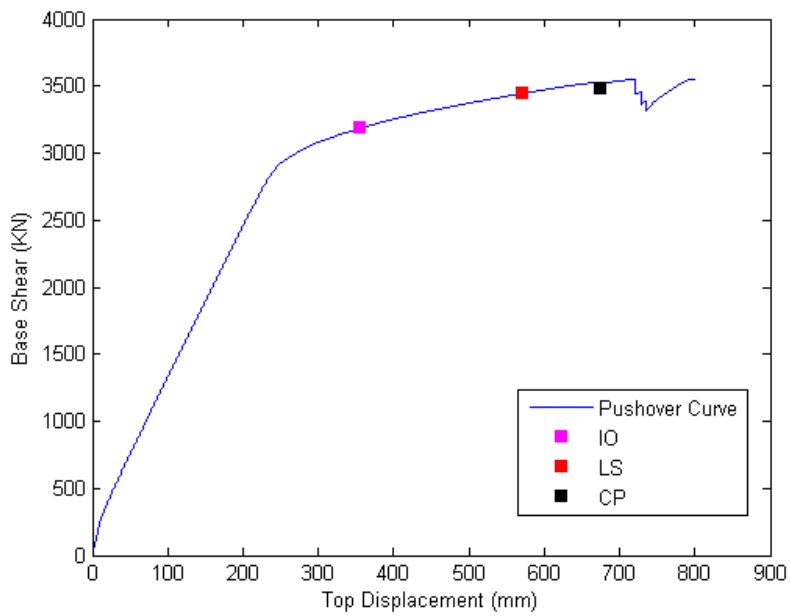


Figure 7. The performance levels for the optimum solution

## 6. INCORPORATING SOIL-STRUCTURE INTERACTION IN OPTIMUM SOLUTION

Seismic rehabilitation standards [20] for buildings located in moderate and high seismic risk zones require consideration of the interaction between the structure and the supporting soil.

FEMA for the seismic rehabilitation of structures allows modeling the foundation by means of a set of uncoupled elasto-plastic springs at the base of the columns and walls.

Considering inertial effects of the soil-structure interaction is accomplished by first method of the FEMA-356. For shallow bearing footings that are rigid with respect to the supporting soil, an uncoupled spring model, as shown in Figure 8, will represent the foundation stiffness.

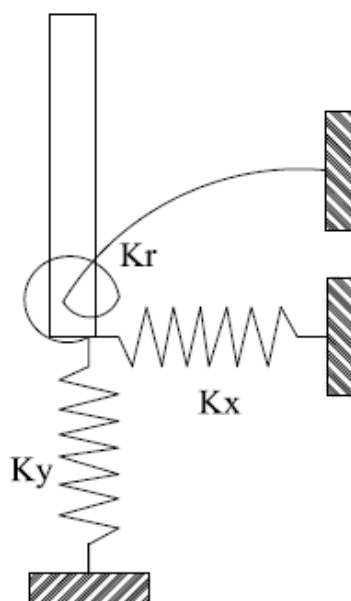


Figure 8. Uncoupled spring model

Properties of the soil under foundation are provided in Table 4. Notations of foundation are specified in Figure 9. Foundation dimensions and stiffness of the springs are in Table 5. These stiffness values are calculated according to the FEMA-356 relationships.

Assessment of the soil-structure effects on optimum solution is under consideration. Elastic soil and elasto-plastic model are considered and compared to the fixed based mode. Comparison of the capacity curves are shown in Figure 10. This plot also shows that the SSI incorporation reduces the base shear force capacity of shear wall and this reduction is more significant for the elasto-plastic soil model. Obviously, considering the SSI leads to an increase in the fundamental period. Fundamental period in the fixed base condition for optimum shear wall is 0.52 sec and it is equal to 0.88 sec after considering the SSI.

Table 4. Soil properties

$c$ (KN/m <sup>2</sup> )	$\phi$	$\nu$	$\gamma$ (kN/m)	$V_s$ (m/s)
0	35	0.35	18	335

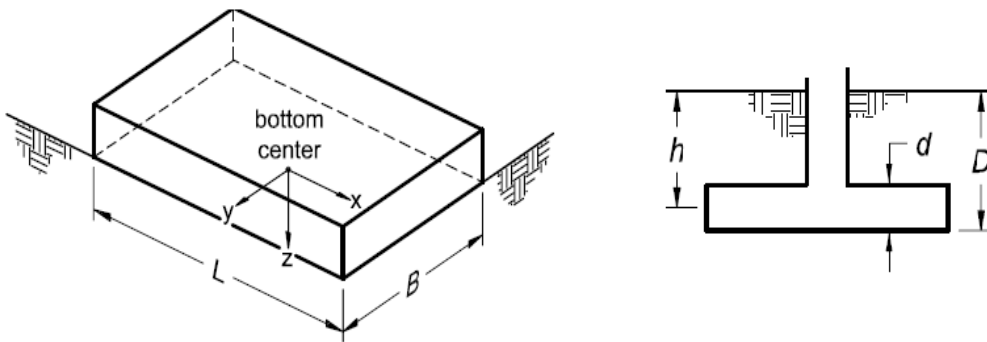


Figure 9. General notations of the foundation

Table 5. Foundation properties

L (m)	B (m)	D (m)	d (m)	$K_{emb\ x}$ (kN/m)	$K_{emb\ y}$ (kN/m)	$K_{emb\ r}$ (kN.m)
7.8	3	1.5	0.8	1.4474 e6	1.4138 e6	1.8787 e7

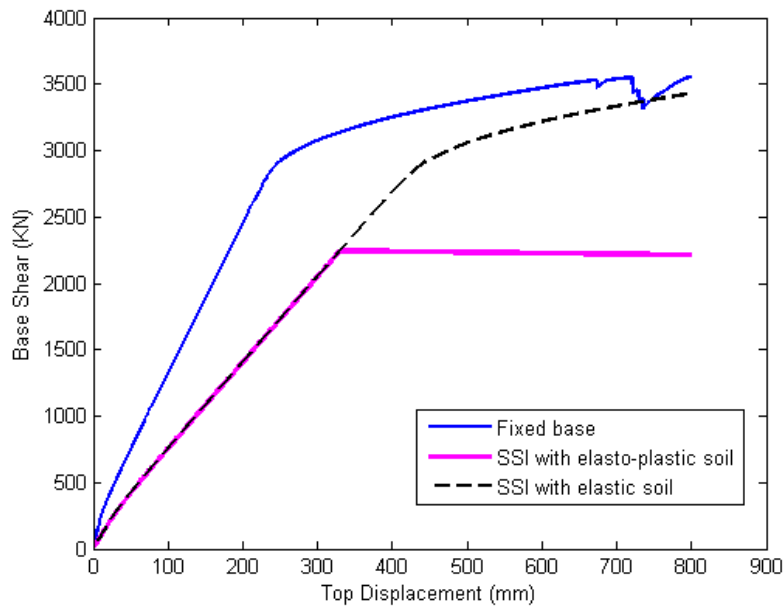


Figure 10. Comparison of the capacity curves in three conditions

### 7. BILINEAR APPROXIMATION OF THE CAPACITY CURVE: AN OPTIMIZATION PROBLEM

In this section, a simple optimization based method is proposed for bilinear approximation of the capacity curve, Figure 11.

According to FEMA provisions [20], the nonlinear force-displacement relationship between base shear and displacement of the control node will be replaced by an idealized relationship. In order to accomplish this idealization: firstly, the area below the original curve  $S_1$  must be equal to the area below OB and BC lines  $S_2$ . Secondly, line of the OB must collide with the original curve in force value of  $0.6V_y$ , i.e. an intersection point like A.

The main steps of the optimization problem are as follows:

- i) Optimization variables are  $V_y$  and  $\delta_y$ . These are variables' limitations:

$$0 < V_y < V_f \quad \text{and} \quad 0 < \delta_y < \delta_t \quad (31)$$

$V_f$  is the failure force of structure.

- ii) Consider  $H(x) = |S_2 - S_1|$  as an objective function that must be minimized. Absolute minimum value of this objective function is equal to zero but a small value near to zero is an admissible solution. Note that  $S_1$  is constant and  $S_2$  is calculated by variables in each iteration. Calculation is based on original curve data and its accuracy relies on the step intervals of the pushover analysis.
- iii) Interpolate  $\delta_{0.6V_y}$  corresponding to  $0.6V_y$  of the original curve.
- iv) Calculate the linear equation of OB from optimization variables in each iteration:

$$OB: V = \left(\frac{V_y}{\delta_y}\right)\delta \quad (32)$$

- v) Construct the constraint of the problem with the value of  $V$  corresponding to Interpolated  $\delta_{0.6V_y}$  which is determined using Eq. (32).

$$constraint = \left| \frac{V}{0.6V_y} - 1 \right| < \varepsilon_0 \quad (33)$$

$\varepsilon_0$  (e.g.  $\varepsilon_0=0.01$ ) is the tolerance value for changing an equality constraint to an inequality constraint.

- vi) Using an optimization algorithm such as CSS for solving problem. The problem is terminated when the objective function has a value near to zero.

Now, the effective stiffness  $K_e$  and  $\alpha K_e$  can be determined as the slope of the OB and the slope of BC, respectively [20].

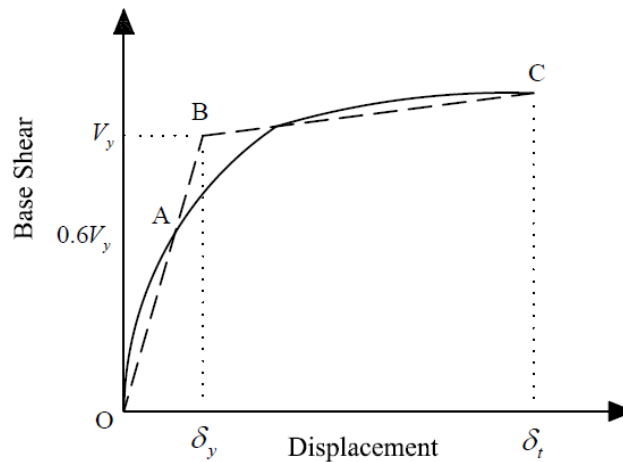


Figure 11. Force-displacement curve and its bilinear approximation

The  $V_y$  and  $\delta_y$  of three conditions are obtained by the optimization process, as shown in Table 6.

Table 6. Bilinear approximation parameters obtained from optimization based method

Condition	$\delta_y$ (mm)	$V_y$ (kN)
Fixed base	279	3272
SSI with Elastic soil	455	3096
SSI with Elasto-plastic soil	280	2124

As we see from Table 6, the SSI effects on  $V_y$  and  $\delta_y$  values are significant. In elastic soil,  $\delta_y$  is greater than the fixed base mode. In elasto-plastic soil this is not much different, but  $V_y$  is more different from fixed base form in comparison with elastic soil model. Since in the elasto-plastic soil we have plastic moment and force limitations, thus in this plastic moment and forces large deformations occur. Hence, energy dissipation exists and the area under the capacity curve of the elasto-plastic model is smaller than the elastic model. This ductility causes the plastic hinges not to be formed in some checkpoints until target displacement of 800 mm.

## 8. CONCLUDING REMARKS

Considering seismic design criteria in structural optimization leads to more efficient structural design optimization, because in seismic design more provisions must be considered to have a safe structure against earthquake. Shear walls are one of the important structural elements that provide lateral bracing for the rest of the structure. In regions with

medium or high seismic risk level, special reinforcement is required in order to have favorable performance of concrete structures against earthquake hazards. Here, special shear wall optimization using the CSS algorithm is presented. A database of shear wall sections is proposed so as to have a practical optimization. Plastic rotation constraint is imposed as a performance constraint. These plastic rotations are obtained from nonlinear static analysis including material and geometry nonlinearity and target displacement is calculated based on the aforementioned convex model of design spectra of the FEMA. After optimization process, optimum shear wall capacity curve and plastic hinge formation are presented. Then the SSI effects are verified and capacity curves are obtained. After that the bilinear approximation of capacity curves as an optimization problem is proposed and specifications of each condition are compared. These methodologies propose a new aspect of special shear wall performance based seismic design optimization and assessment.

## REFERENCES

1. Kaveh A, Sabzi O. A comparative study of two meta-heuristic algorithms for optimum design of reinforced concrete frames. *Int J Civil Eng*, 2011; **9**(3):193–206.
2. Sarma KC, Adeli H. Cost optimization of concrete structures. *J Struct Eng, ASCE*, 1998; **124**(5) :570–78.
3. Wight JK, Macgregor JG. *Reinforced Concrete: Mechanics and Design*. 6<sup>th</sup> ed. New Jersey: Pearson Education, 2012.
4. Mostofinejad D. *Reinforced Concrete Structures*, Vol 2. Esfahan: Arkan Danesh; 2009.
5. Wallace JW. Seismic design of RC structural walls, part I: new code format. *J Struct Eng, ASCE*, 1995; **121**(1):75-87.
6. Wallace JW. Seismic design of RC structural walls, part II: Applications. *J Struct Eng, ASCE*, 1995; **121**(1):88-101.
7. Sasani M. A two-level-performance-based design of reinforced concrete structural walls. Proceedings of 6th US National Conference on Earthquake Engineering, EERI: Oakland, CA, 1998.
8. Kowalsky MJ. RC structural walls designed according to UBC and displacement-based methods. *J Struct Eng, ASCE*, 2001; **127**(5):506–16.
9. Saka MP. Optimum design of multistory structures with shear walls. *Comput Struct*, 1991; **44**(4):925–36.
10. Ganzerli S, Pantelides CP, Reaveley LD. Performance-based design using structural optimization. *Earthquake Eng Struct Dyn*, 2000; **29**:1677–90.
11. Cheng FY, Pantelides CP. Combining Structural Optimization and structural control. Technical Report, NCEER 88-006, State University of New York, Buffalo, January; 1988.
12. Fragiadakis M, Papadrakakis M. Performance-based optimum seismic design of structural reinforced concrete structures. *Earthquake Eng Struct Dyn*, 2008; **37** :825–44
13. Grange S, Kotronis P, Mazars J. A macro-element to simulate dynamic soil-structure interaction. *Eng Struct*, 2009; **31**: 3034–46.
14. Hall Jr. JR. Coupled rocking and sliding oscillations of rigid circular footings, in:

International symposium on wave propagation and dynamic properties of earth materials, Albuquerque, 1967.

15. Parmelee RA. Building-foundation interaction effect. *J Eng Mech, ASCE*, 1967; **93**(EM2): 131–52.
16. Parmelee RA, Perelma DS, Lee SL, Keer ML. Seismic response of structure foundation systems. *J Eng Mech, ASCE*, 1968; **94**(EM6): 1295–315.
17. Paul Smith-Pardo J. Design aids for simplified nonlinear soil-structure interaction analyses. *Eng Struct*, 2012; **34**: 572–80.
18. Ghersi A, Massimino MR, Maugeri M. Non-Linear moment–rotation relationship at the base of shear walls, 12WCEI 2000.
19. Raychowdhury P. Seismic response of low-rise steel moment-resisting frame (SMRF) buildings incorporating nonlinear soil-structure interaction (SSI). *Eng Struct*, 2011; **33**: 958–67.
20. Fema-356. Prestandard and commentary for seismic rehabilitation of buildings. Federal Emergency Management Agency: Washington, DC, 2000.
21. Lee C, Ahn J. Flexural design of reinforced concrete frames by genetic algorithm. *J Struct Eng, ASCE*, 2003; **129**(6):762–74.
22. American Concrete Institute (ACI). Building code requirements for structural concrete and commentary. ACI 318-08, 2008.
23. Minimum design loads for building and other Structures, ASCE 7-10. 2010.
24. Ben-Heim Y, Elishako I. *Convex Models of Uncertainty in Applied Mechanics*, Elsevier: New York, 1990.
25. Kaveh A, Talatahari S. A novel heuristic optimization method: charged system search. *Acta Mech*, 2010; **213**: 267–89.
26. Kaveh A, Talatahari S. A charged system search with a fly to boundary method for discrete optimum design of truss structures, *Asian J Civil Eng*, 2010; **11**(3): 277–93.
27. Kaveh A, Talatahari S. Charged system search for optimal design of frame structures. *Appl Soft Comput*, 2012; **12**: 382–93.
28. The Language of Technical Computing. MATLAB: Math Works Inc; 2007.
29. McKenna F, Fenves GL. et al. Open system for earthquake engineering simulation (OpenSees) 2.2.2; 2010. <http://www.opensees.berkeley.edu>.
30. Thomas TC, Hsu YL, Mo T. *Unified Theory of Concrete Structures*, John Wiley & Sons Ltd; 2010.